DJS Vol. 48(1)(2024) –pp.145-157 ISSN: 1012-5965

Delta Journal of Science
Available online at
https://djs.journals.ekb.eg/

Research Article

PHYSICS

FTIR, DC electrical measurements of Mg Nano-ferrite and their composites with reduced graphene oxide (rGO) and polypyrrole (PPy)

Bilal Ibrahim*, Maha K. Omar, Samia A. Saafan, R.E. El Shater

Physics Department, Faculty of Science, Tanta University, Tanta 31527, Egypt

***Correspondence**: Bilal Ibrahim **E-mail:** Bilal.Ibrahim@science.tanta.edu.eg

Received: 21/2/2024 **Accepted:** 21/3/2024

KEY WORDS

Structural properties; X-ray diffraction; Energy dispersive x-ray; DC conductivity; Activation energy.

ABSTRACT

Mg ferrite nanoparticles have been synthesized using the citrate-nitrate auto-combustion technique. Also, polypyrrole (PPy) has been synthesized using a chemical polymerization technique. Physically blending ferrite with PPy and/or rGO in various ratios has produced composite samples. The XRD indicates that the ferrite nanoparticles are in a crystalline state with lattice constant 0.845 A and crystallite size 40 nm, and the composite samples contain PPy and rGO as intended. FTIR analyses indicate vibrational modes of octahedral at 405cm^{-1} and tetrahedral mode at 565 cm^{-1} of spinel structure. The EDX analysis of Fe, Mg, O, C, and N verified the chemical composition of pure ferrite and its composites. DC conductivity has been measured for all samples as a function of temperature. The ferrite/PPy composite samples exhibit greater DC conductivity compared to the pure ferrite sample and the ferrite/rGO sample. The composite of $MgFe_2O_4$/10% rGO/10% PPy exhibits exceptional conductivity due to the strong π-π stacking interaction between rGO and PPy. This interaction allows for the generation of a greater number of delocalized electrons within their structure, consequently reducing the hindrances to electron mobility and facilitating a more effortless flow of electrons. Moreover, within this composite, which comprises PPy and rGO, these effects are particularly pronounced. Therefore, $MgFe_2O_4$/10% rGO/10% PPy has the smallest activation energy among all samples (0.145 eV).

Introduction

The dynamic performance of spinel ferrite makes it a very appealing ferrite material **(Mulushoa et al., 2018)**. It is used in data storage devices, microwave absorption materials, ferrofluid and catalysis, gas sensing materials, anode materials of lithium-ion batteries, magnetic hyperthermia, optical and dielectric materials, and more **(Babu et al., 2017; Himakar et al., 2021; Mercy et al., 2020; Mulushoa et al., 2019).** Usually, researchers use simpler and more effective synthesis approaches for the synthesis of magnetic materials, their modification, and their characterization **(Madhavilatha et al., 2022; Sakthipandi et al., 2022; Bharathi et al., 2023).** Spinel ferrites have excellent magnetic characteristics in a variety of disciplines, including recording, imaging, medication delivery, detoxification, etc (**Ahilandeswari et al.**, **2020**; **Packiaraj et al.**, **2020**). Magnesium ferrite ($MgFe_2O_4$) is a spinel ferrite that has a hysteresis loop of significant magnetic properties. This makes it perfect for memory, switching circuits, and low-loss microwave devices (**Wang et al.**, **2022**). $MgFe_2O_4$ ferrite has also been employed in gas sensors (**George et al.**, **2021**), heterogeneous catalysts (**Sheykhan et al.**, **2012**)**,** and humidity sensors (**Kuru et al.**, **2020**)**,** as well as for their photoelectric properties (**Kumar et al.**, **2020**).

Also, polymer-based composites have found extensive usage in various fields, such as rechargeable batteries (**Liu et al.**, **2014**), corrosion-resistant machinery (**Madhusudhan et al.**, **2022**), and microwave absorption materials (**Velhal et al.**, **2019**). From which conducting polymers like polypyrrole (PPy), and polyaniline (PANI) have gained significant attention. These remarkable subsstances not only possess the remarkable ability to conduct electricity but also exhibit cost-effectiveness and ecological stability, positioning them as a groundbreaking category of materials. Adding magnetic fillers, such as ferrites, can improve the electromagnetic characteristics of conducting polymers, increasing their effectiveness in some applications. Making PPy-based nanocomposite ferrites has many benefits (**Radhakrishnamurty et al.**, **1978**), including being cost-effective, having a high energy and remanence content, and being very resistant to corrosion. Also, incorporating metal oxide materials like ferrites into the graphene matrix enhances performance for various applications. These nanocomposites enable the generation of electrical energy with remarkable power density, thus playing a crucial role in developing energy devices and optoelectronics (**Hiralal et al.**, **2016**; **Kant et al.**, **2022**).

Here in the present study, the structural, morphological characteristics using XRD, EDX and FTIR and DC electrical properties of sol gel auto-combustion magnesium ferrite and its composites with rGO and PPy were investigated. Physical mixing had been carried out by sonication process. All composites have been prepared in the same conditions. Additionally, the DC conductivity of nanocomposites was examined at varying temperatures.

Experimental Methods

Synthesis procedure and chemicals

The pure-phase $MgFe_2O_4$ has been produced utilizing an inexpensive and chemical-based auto-combustion method (**Prasad et al.**, **2023**). The high-purity reactant chemicals used were Mg $(NO_3)_2.6H_2O$ with a purity (98%), Fe $(NO_3)_3.9H_2O$ with a Purity (98%) and citric acid with a purity (99.5%), which have been purchased from Loba Chemie. Mg $(NO_3)_2.6H_2O$ and Fe $(NO_3)_3.9H_2O$ solutions in distilled water have been mixed with the citric acid solution. At room temperature, ammonia (NH_4OH) has been added drop by drop to the nitrate-citrate solution to change the pH to 6.0. This made the solution darker and thicker. The water was then evaporated on a hot plate, resulting in the formation of a viscous gel. With much more heating, a self-propagating combustion event began within the gel. The combustion continued until the entire gel was transformed into a charred ash-like powder. The rough powder was then ground in an agate mortar to produce a fine powder. The fine powder was sintered for 6 hours at 900 °C then left into the furnace until being cooled to room temperature.

The pure PPY sample was created via chemical polymerization of pyrrole monomer with apurity (99.5%), which have been purchased from Sisco Research laboratories, (with $FeCl_3.6H_2O$ as an oxidizing agent) with a ratio of pyrrole: $FeCl_3$ equals 1:2.33. A solution of 1.21 mole of ferric chloride was added drop by drop to 0.52 mole of pyrrole monomers. The resultant precipitate was obtained after 24 hours by filtering and washing with distilled water until it became clear (**Diauudin et al.**, **2020**). The reduced graphene oxide was bought from Nano-Gate- Cairo - Egypt. We prepared the composites by physically mixing weight ratios carried out by the sonication process and grinding them into fine powders in an agate mortar for three hours. All composites have been prepared in the same conditions.

Characterization

Fourier transform infrared (FTIR) spectra for all samples have been recorded by Bruker FT-IR in the range of 400–2000 cm^{-1} at room temperature. Also, the prepared sample's structure has been investigated by XRD (German Bruker D8 advance diffractometer, Ultima IV-XRD) ($10^{\circ} \leq 2\theta \geq 80^{\circ}$, Cu-Kα, λ = 1.5405 Å). Energy-dispersive X-ray spectroscopy (EDXS) has also been used to study the element compositions of the prepared samples. Electrical properties have been evaluated using a four-probe methodology with a programmable electrometer for DC measurements. The DC conductivity of the samples was analyzed as a function of temperature, encompassing a range from 303 K to 423 K.

Result and discussion

XRD

The X-ray diffraction method confirmed the crystalline nature of the synthesized nanoparticles. Fig. 1 (a–f) shows the XRD patterns. The obtained peaks of magnesium ferrite particles are matched with the standard JCPDS card (no. 790416). The observed diffractogram patterns of all the samples verified the existence of a single-phase spinel ferrite with no additional unwanted peaks. The 2θ values of 30.74◦, 36.1◦, 43.74◦, 54.11◦, 57.62◦, and 63.27◦ are the characteristic angles for the standard peaks of spinel cubic ferrites. These values correspond to the reflection from the (220), (311), (222), (400), (422), (511), and (440) planes (JCPDS no. 790416) (**Swati et al.**, **2021**), as shown in the $MgFe_2O_4$ standard card. Also, the peaks characteristic of PPy and rGO are not obviously seen in Fig. 1. This could be because the ratios of the polymer and reduced graphene oxide in the studied composites aren't very high compared to the ratios of the ferrite, along with the much higher intensity of the ferrite peaks making them much more noticeable than the peaks of PPy and rGO.

FT-IR spectra

As demonstrated in Fig. 2 (a–f), the absorption bands below 600 cm^{-1} indicate the presence of pure ferrite. Specifically, the higher band υ_1 at 565 cm^{-1} shows bond stretching vibrations of metal ions placed at the tetrahedral sites Fe-O, whereas the lower band υ_2 at 405 cm^{-1} relates to bond stretching vibrations of divalent metal ions at the octahedral sites Mg-O. Ferrites have distinct bands around the υ_1 and υ_2 values. As a result, our findings support the development of the required ferrite, which is consistent with previous research. The FTIR analysis of the PPy composite reveals distinct absorption band around 933.96 cm^{-1} attributable to pyrrole C-H wagging **(Karthikeyan et al.**, **2021**; **Ravikiran et**

al., **2023**). Also, in Fig. 2, the reduced graphene oxide composite is characterized by the presence of two closely positioned peaks around 1078.02 cm^{-1} and 1460.50 cm^{-1}, which are usually related to the C-O-C and C-O, respectively (**Folorunso et al.**, **2022**; **Alrefaee et al.**, **2023**). The pronounced band at 3386.42 cm^{-1} may be associated with the symmetric stretching vibrations of OH groups (**Folorunso et al.**, **2022**; **Sharma et al.**, **2023**).

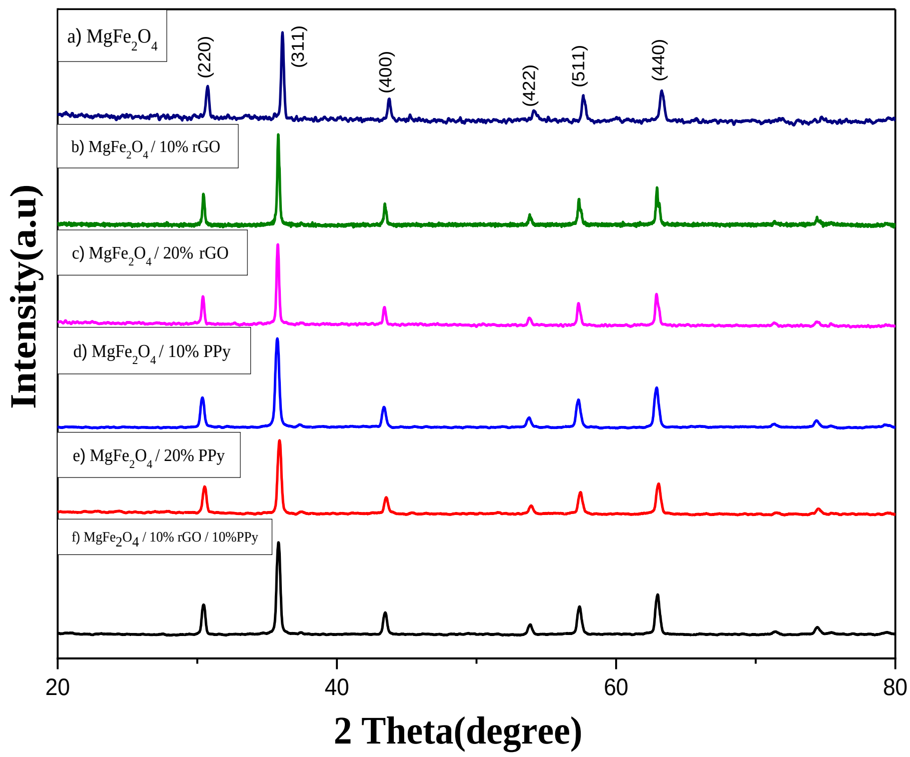

Fig. (1): (a–f) X-ray diffraction patterns of nanocomposite samples

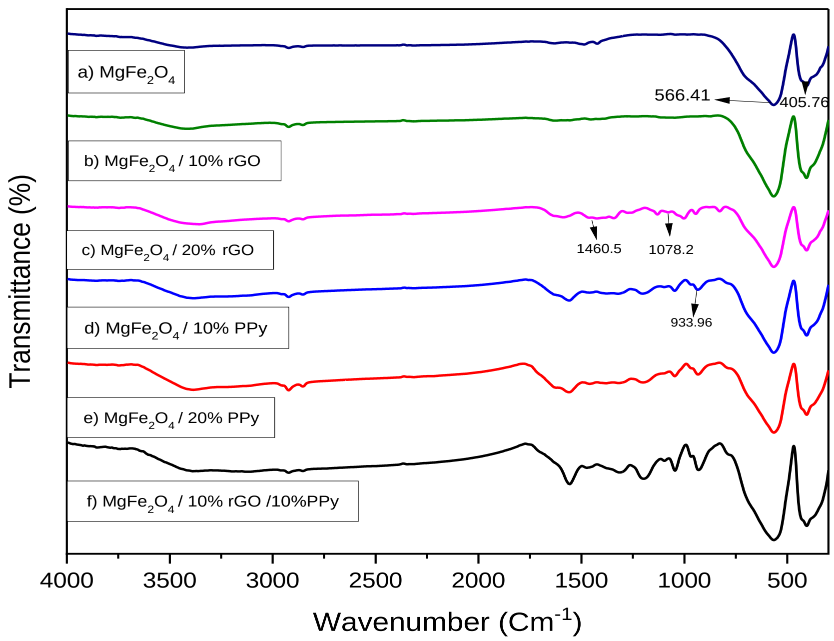

Fig. (2): (a–f) FTIR spectra of nanocomposite samples.

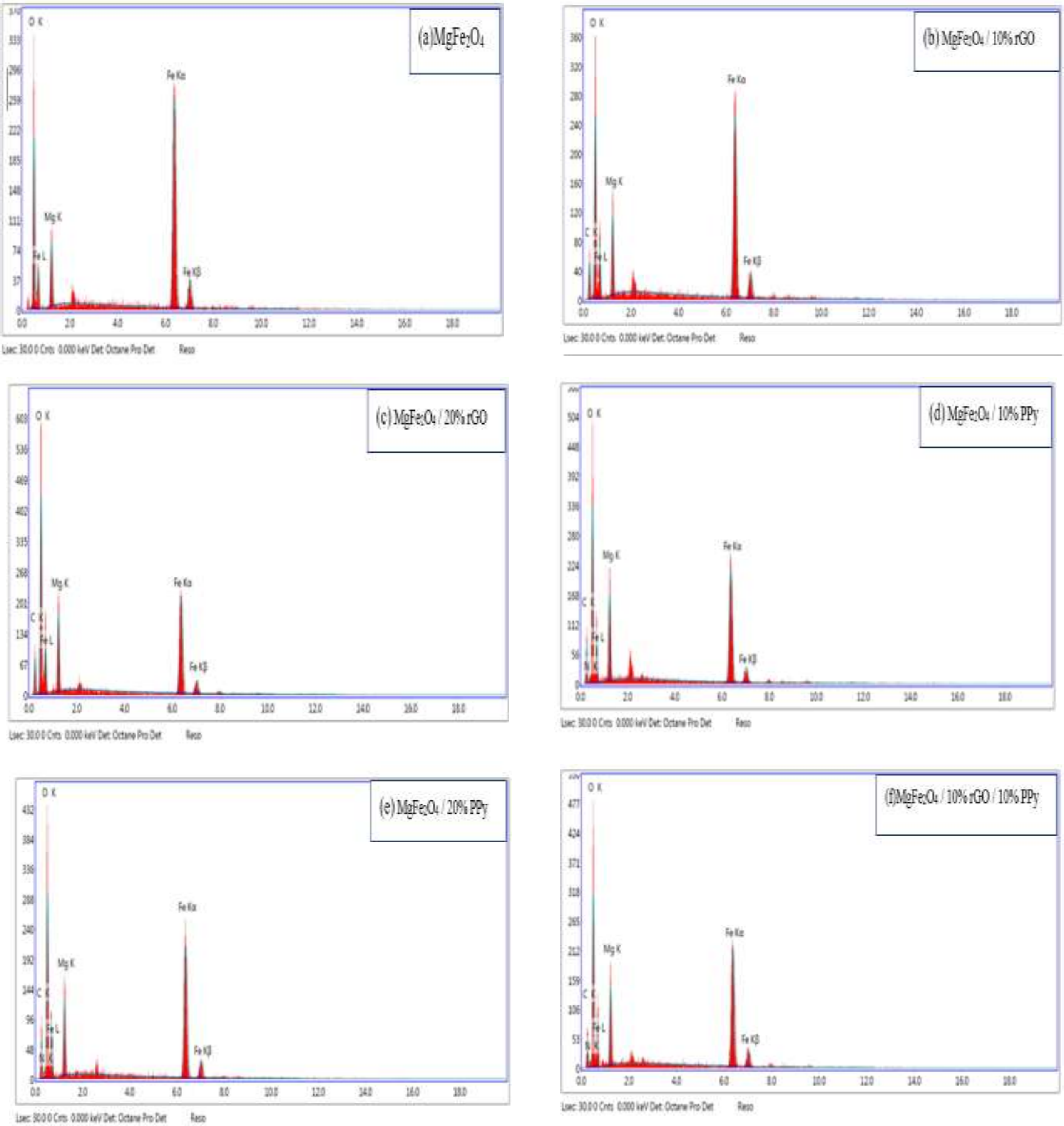

Fig. (3): (a–f) EDX patterns of the composites.

Energy-dispersive X-ray (EDX)

The EDX patterns are shown in Fig. 3 (a–f), confirming the proper chemical compositions of the prepared ferrite sample and their composite samples with their intended elemental ratios. It is evident from Fig. 3 (a–f) that only elemental contents of Mg, C, N, Fe, and O are present in the EDX spectra of nanoparticles. Furthermore, the absence of impurity peaks in the EDX spectra of samples showed that there is no impurity atom present in these nanoparticles, confirming the high purity of the synthesized nanoparticles.

DC Conductivity (σ_{dc})

The DC conductivity of composites was measured using pellet samples to analyze some of the electrical properties of the synthesized materials. The conductivity of the composites was calculated from the measured current value by taking the thickness and diameter of the sample pellets into account. As shown in Fig. 4, the DC conductivity of the composites increases as the temperature rises from 303 K to 423 K, indicating that the prepared composites have a semiconducting behavior. In ferrites, the process of conduction occurs by an electron transfer from a divalent ion to a trivalent ion of the same element at the same site. While the charge may be transferred in conducting polymers most probably via polaron interchain motion (**Swati et al.**, **2021**). Charge carriers follow hopping mechanisms in all scenarios, requiring activation energy that increases with temperature to move to adjacent sites. Therefore, the decrease in oxygen sites on reduced graphene oxide (rGO) results in enhanced conductivity. The reduced graphene oxide sheets, which are located close to one another at a distance of less than or equal to 10 angstroms, may also have an impact on the direct current conductivity (**Singh et al.**, **2018**). The data from the linearly fitted ln σ vs. 1000/T plot follows the Arrhenius equation.

$$\sigma_{dc} = \sigma_0 \exp\left(\frac{-E}{KT}\right)$$

where σ_o is constant, E is the activation energy for DC conduction, k is Boltzmann's constant, and T is the absolute temperature. By taking the logarithm to the natural base e:

$$\ln \sigma_{dc} = \frac{-E}{KT} + constant$$

The reason why conductivity goes up as temperature goes up is because thermal energy makes it easier for charge carriers to move around in the hopping-based conduction mechanism. The activation energy reflects the energy needed to cross the potential barrier associated with the location of the charge carrier, and it can be deduced from the slope of each fitted line. Table (1) demonstrates that the pure ferrite sample has the highest activation energy among the samples due to its relatively poor conductivity. The activation of PPy composites is always lower than that of rGO composites at the same ratio, owing to PPy's higher conductivity. Strong π-π stacking interactions between rGO and PPy can make more electrons spread out in their lattice and lower the barriers to electron movement, which makes it easier for electrons to move (**Ravikiran et al., 2023**). It is worth mentioning that for the composite containing PPy and rGO, there are two activation energies in two ranges of temperature which may be due to the strong π-π stacking interactions mentioned above between rGO and PPy which is expected to be stronger at lower temperature than at high temperature.

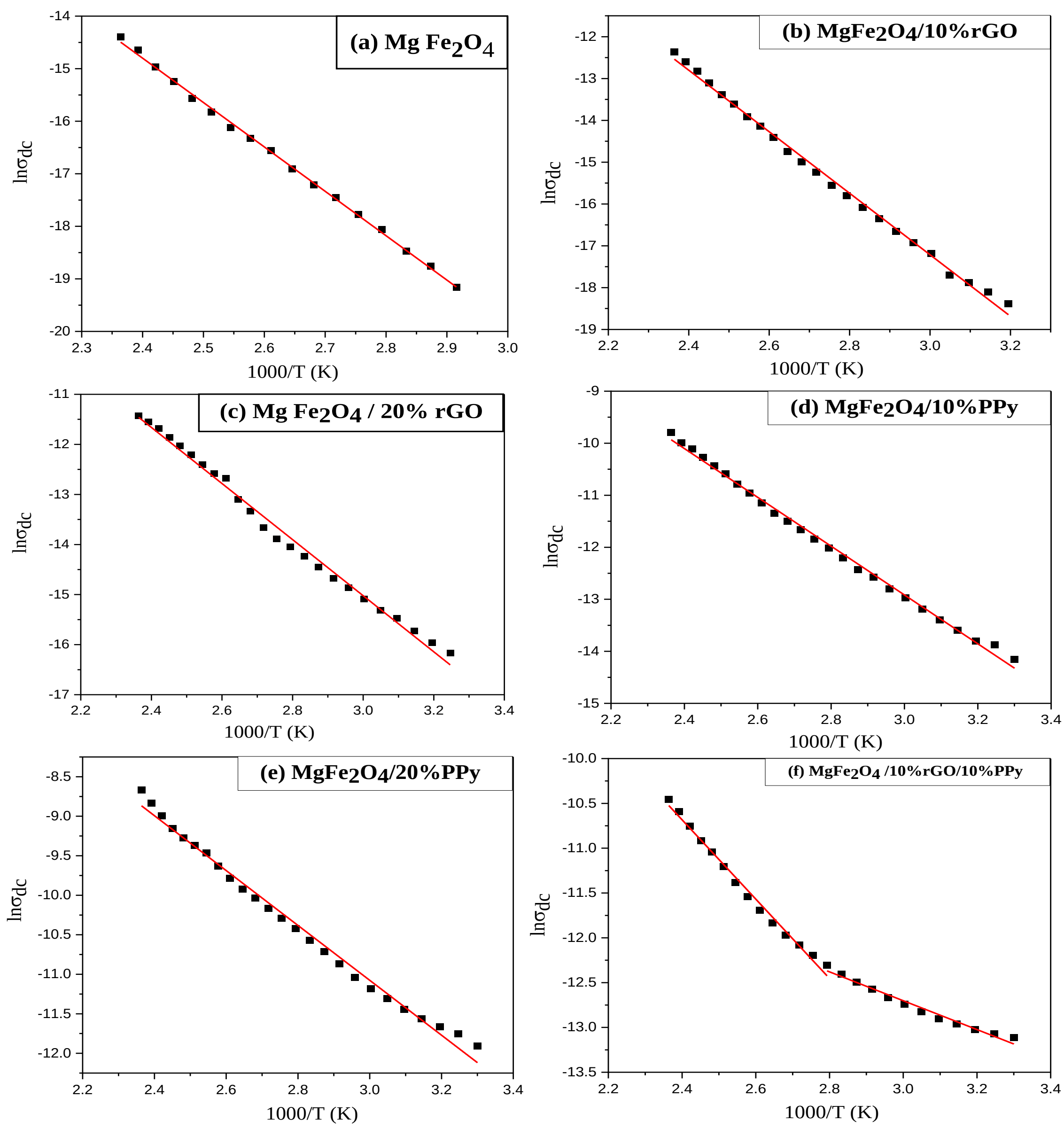

Fig. (4): (a-f) The temperature dependence of DC conductivity of the samples with linear fit.

Table (1): Activation energy of DC conductivity by using Arrhenius relation

Sample	**$MgFe_2O_4$**	**$MgFe_2O_4$/ 10% rGO**	**$MgFe_2O_4$/ 20% rGO**	**$MgFe_2O_4$/ 10% PPy**	**$MgFe_2O_4$/ 20% PPy**	**$MgFe_2O_4$/ 10%PPy/10%rGO**
Activation energy	**0.728**	**0.٦٥٨**	**٠.٤٥٩**	**٠.٤٠٩**	**٠.٣٤١**	**٠.٣٩٤/ 0.145**

Conclusions

$MgFe_2O_4$ nanoparticle could be successfully synthesized via the auto combustion method. X-ray studies confirm the formation of single-phase spinel structure. FTIR studies have revealed the presence of the two main absorption bands of the ferrite (υ_1 and υ_2) around 565.25 cm^{-1} and 405.83 cm^{-1} and the main bands of PPy and rGO. EDX analysis confirms the presence of the intended elements in the samples. The σ_{dc} of the ferrite and the composites as a function of temperature has exhibited a semiconducting behavior. Also, the σ_{dc} has increased with the increasing PPy and rGO content in the ferrite samples. Composites containing polypyrrole show greater values of conductivity than those of composites containing reduced graphene oxide. $MgFe_2O_4$/10% rGO/10% PPy has the best conductivity because rGO and PPy have a strong π-π stacking interaction that may create more delocalized electrons in their lattice and lower the barriers to electron movement, making it easier for electrons to move around. Moreover, for this composite (containing PPy and rGO), there are obviously two activation energies in two ranges of temperature which may confirm the above mentioned strong π-π stacking interactions which is expected to be stronger at lower temperature than at high temperature.

Reference

Ahilandeswari, E., Rajesh Kanna, R. and Sakthipandi, K. (2020), Synthesis of Neodymium-Doped Barium Nanoferrite: Analysis of Structural, Optical, Morphological, and Magnetic Properties. *Phys. B Condens. Matter*, 599(July): 412425. https://doi.org/10.1016/j.physb.2020.412425

Ahilandeswari, E., Sakthipandi, K., Rajesh Kanna, R., Hubálovská, Marie and Vigneswaran, D. (**2022**), Lanthanum Substitution Effect on the Structural, Optical, and Dielectrical Properties of Nanocrystalline BaFe2O4 Ferrites. *Phys. B Condens. Matter*, 635(December 2021).

Alrefaee, Salhah H., Trabelsi, Amira Ben Gouider, Abdelhamid, Ahmed E., Ward, Azza A., Elsharkawy, Wafaa, Alkallas, Fatemah H., Mostafa,

Ayman M., Al-Ahmadi, Ameenah N., Nafee, Sherif S., Adel Pashameah, Rami and Khalil, Ahmed M. (**2023**), Recycled Polystyrene/Polyvinylpyrrolidone/Reduced Graphene Oxide Nanocomposites for Optoelectronic Devices. *J. Mater. Res. Technol.*, 25: 2631–2640. https://doi.org/10.1016/j.jmrt.2023.05.249

Babu, V. Ramesh and M. P., Dr. Soni (**2017**), Modelling of Twin Rotor Axial Flux Induction Machine and Its Application as Differential in Electrical Vehicles. , 5(5): 118–127.

Diauudin, Farah Nabila, Aminah, Siti, Noor, Mohd, Izuan, Jahwarhar, Rashid, Abdul, Knight, Victor Feizal, Zin, Wan, Yunus, Wan, Ong, Keat Khim, Azilah, Noor, Kasim, Mohd, Taufik, Safura, Samsuri, Alinda, Shamsudin, Intan Juliana and Latip, Wahhida (**2020**), Preparation and Characterisation of Polypyrrole-Iron Oxyhydroxide Nanocomposite as Sensing Material. , 2020.

Folorunso, Oladipo, Kumar, Neeraj, Hamam, Yskandar, Sadiku, Rotimi and Ray, Suprakas Sinha (**2022**), Facile Solvent/Drying Fabrication of PVA/PPy/RGO: A Novel Nanocomposite for Energy Storage Applications. *Results Mater.*, 15(June): 100295. https://doi.org/10.1016/j.rinma.2022.100295

George, Jacob and Abraham, K. E. (**2021**), Gas Sensing Characteristics of Magnesium Ferrite and Its Doped Variants. *Phys. B Condens. Matter*, 610(March): 412958. https://doi.org/10.1016/j.physb.2021.412958

Himakar, P., Jayadev, K., Parajuli, D., Murali, N., Taddesse, Paulos, Mulushoa, S. Yonatan, Mammo, Tulu Wegayehu, Kishore Babu, B., Veeraiah, V. and Samatha, K. (**2021**), Effect of Cu Substitution on the Structural, Magnetic, and Dc Electrical Resistivity Response of Co0.5Mg0.5-XCuxFe2O4 Nanoferrites. *Appl. Phys. A Mater. Sci. Process.*, 127(5): 1–10. https://doi.org/10.1007/s00339-021-04521-w

Hiralal, Pritesh, Rius, Gemma, Yoshimura, Masamichi and Amaratunga, Gehan A.J. (**2016**), Graphene-Based Electrochemical Capacitors. *Graphene Sci. Handb.*, 5–6(1): 479–494.

Jesus Mercy, Shaik, Murali, N., Ramakrishna, A., Ramakrishna, Y., Veeraiah, V. and Samatha, K. (**2020**), Microstructural, Thermal, Electrical and Magnetic Analysis of Mg2+ Substituted Cobalt Ferrite. *Appl. Phys. A Mater. Sci. Process.*, 126(11). https://doi.org/10.1007/s00339-020-04048-6

Kant, Ravi, Sharma, Divya and Chanchal, Vageesha (**2022**), Enhancement in Dielectric and Optical Properties of Al Doped ZnO/ Reduced Graphene Oxide Nanocomposite. *Mater. Technol.*, 37(8): 655–662. https://www.tandfonline.com/doi/full/10.1080/10667857.2020.1868745

Karthikeyan, Perumal, Elanchezhiyan, S. SD, Meenakshi, Sankaran and Park, Chang Min (**2021**), Magnesium Ferrite-Reinforced Polypyrrole Hybrids as an Effective Adsorbent for the Removal of Toxic Ions from Aqueous Solutions: Preparation, Characterization, and Adsorption Experiments. *J. Hazard. Mater.*, 408(August 2020): 124892. https://doi.org/10.1016/j.jhazmat.2020.124892

Kuru, Mehmet, Kuru, Tuğba Şaşmaz, Karaca, Ertuğrul and Bağcı, Sadık

(**2020**), Dielectric, Magnetic and Humidity Properties of Mg–Zn–Cr Ferrites. *J. Alloys Compd.*, 836.

Liu, Y., Zhang, B. H., Xiao, S. Y., Liu, L. L., Wen, Z. B. and Wu, Y. P. (**2014**), A Nanocomposite of MoO3 Coated with PPy as an Anode Material for Aqueous Sodium Rechargeable Batteries with Excellent Electrochemical Performance. *Electrochim. Acta*, 116: 512–517.

Madhavilatha, B., Parajuli, D., Jayadev, K., Komali, Ch, Murali, N., Veeraiah, V. and Samatha, K. (**2022**), Effect of Cu Substitution on Magnetic Properties of Co0.6Ni0.4Fe2O4 Nanoferrites. *Biointerface Res. Appl. Chem.*, 12(2): 1899–1906.

Madhusudhan, C. K., Mahendra, K., Raghavendra, Narasimha, Revanasiddappa, M. and Faisal, Muhammad (**2022**), Corrosion-Resistant Polypyrrole-Banana Carbon (PPy-BC) Nanocomposites for Protection against Electromagnetic Interference: A Green Approach. *J. Mater. Sci. Mater. Electron.*, 33(3): 1366–1382. https://doi.org/10.1007/s10854-021-07466-1

Mulushoa, S. Yonatan, Kumari, Ch Vijaya, Raghavendra, Vemuri, Babu, K. Ephraim, Murthy, B. S.N., Suribabu, Kundavarapu, Ramakrishna, Y. and Murali, N. (**2019**), Effect of Zn–Cr Substitution on the Structural, Magnetic and Electrical Properties of Magnesium Ferrite Materials. *Phys. B Condens. Matter*, 572(July): 139–147. https://doi.org/10.1016/j.physb.2019.07.057

Packiaraj, G., Sakthipandi, K. and Hossain, Aslam (**2020**), Effect of 200 MeV Ag16+ Swift Heavy Ion Irradiation on Structural and Magnetic Properties of M-Type Barium Hexaferrite. *Mater. Res. Express*, 7(1).

Packiaraj, G., Sakthipandi, K., Jotania, Rajshree B. and Hossain, Aslam (**2020**), Dielectric and Magnetic Properties of Polyaniline-Blended Y-Type Ba2Ni2Fe12O22 Hexaferrite Composites. *J. Electron. Mater.*, 49(5): 3317–3324. https://doi.org/10.1007/s11664-020-08051-8

Prasad, S. A.V., Srinivas, Ch, Jeevan Kumar, R., Ranjith Kumar, E., Vijaya Babu, K., Meena, Sher Singh, Bhatt, Pramod, Yusuf, S. M. and Sastry, D. L. (**2023**), Study of Thermal, Structural, Microstructural, Vibrational and Elastic Properties of MnxMg0.8–XZn0.2Fe2O4 (0.1 ≤ X≤ 0.7) Ferrite Nanoparticles. *Ceram. Int.*, 49(12): 20419–20428. https://doi.org/10.1016/j.ceramint.2023.03.170

Radhakrishnamurty, C, Likhite, S D and Sahasrabudhe, P W (**1978**), In Situ Magnetic Measurements on Igneous Rock Bodies. *Proc. Indian Acad. Sci. A, Earth Planet. Sci.*, 87: 245–254.

Ravikiran, Y. T., Chethan, B., Prasad, V., Raj Prakash, H. G., Prashantkumar, M., Tiwari, Santosh K. and Thomas, S. (**2023**), Polypyrrole/Reduced Graphene Oxide Composite as a Low-Cost Novel Sensing Material for Fast-Response Humidity Sensor. *Mater. Chem. Phys.*, 303(April): 127800. https://doi.org/10.1016/j.matchemphys.2023.127800

S. Kuswanth Kumar, N. Murali, D. Parajuli, A. Ramakrishna, P. S. V. Subba Rao, M. P. Rao (**2020**), Magnetic and DC Electrical Resistivity Properties of Cu Doped Mg0. 6-XNi0. 4CuxFe2O4 Ferrite. *Solid State Technol.*, 63(5): 4069–4077. http://solidstatetechnology.us/index.ph p/JSST/article/view/5283

Sakthipandi, K., Ganesh Babu, B., Rajkumar, G., Hossian, Aslam, Srinidhi Raghavan, M. and Rajesh Kumar, M. (**2022**), Investigation of Magnetic Phase Transitions in Ni0.5Cu0.25Zn0.25Fe2-XLaxO4 Nanoferrites Using Magnetic and in-Situ Ultrasonic Measurements. *Phys. B Condens. Matter*, 645(August): 414280. https://doi.org/10.1016/j.physb.2022.414280

Sharma, Arti, Jain, Pragyan, Bajpai, Rakesh, Patel, Prabhat and Tiwari, Ashish (**2023**), Synthesis of Ultra-Thin Graphene Oxide/ Reduced Graphene Oxide Nanocomposites and Examine Their Properties. *Mater. Today Proc.*, (xxxx). https://doi.org/10.1016/j.matpr.2023.03.381

Sheykhan, Mehdi, Mohammadnejad, Hossein, Akbari, Jafar and Heydari, Akbar (**2012**), Superparamagnetic Magnesium Ferrite Nanoparticles: A Magnetically Reusable and Clean Heterogeneous Catalyst. *Tetrahedron Lett.*, 53(24): 2959–2964. http://dx.doi.org/10.1016/j.tetlet.2012.03.069

Singh, Fateh, Chandra, Sarita, Panwar, Varij, Uniyal, Divya, Kalra, G S and Kumar, Vinay (**2018**), Diamond & Related Materials Conduction Pathways in CNF / PTFE Composite : Air Oxidized CNFs Coated with the Incomplete Layer of PTFE. *Diam. Relat. Mater.*, 89(August): 227–238. https://doi.org/10.1016/j.diamond.2018.08.015

Swati, Saini, Monika, Anupama and Shukla, Rajni (**2021**), Investigation of Structural, Thermal, and Electrical Properties of Magnesium Substituted Cobalt Ferrite Reinforced Polyaniline Nanocomposites. *Ceram. Int.*, 47(23): 33835–33842. https://doi.org/10.1016/j.ceramint.2021.08.295

Velhal, Ninad, Patil, N. D., Kulkarni, Gopal, Shinde, S. K., Valekar, N. J., Barshilia, H. C. and Puri, Vijaya (**2019**), Electromagnetic Shielding, Magnetic and Microwave Absorbing Properties of Polypyrrole/Ba0.6Sr0.4Fe12O19 Composite Synthesized via in-Situ Polymerization Technique. *J. Alloys Compd.*, 777: 627–637. https://doi.org/10.1016/j.jallcom.2018.11.041

Vijaya Bharathi, Rentapalli, Raju, M. K., Uppugalla, Susmitha, Raghavendra, Vemuri, Parajuli, D., Suryanarayana, B., Yonatan Mulushoa, S., Murali, N. and Samatha, K. (**2023**), Cu2+ Substituted Mg-Co Ferrite Has Improved Dc Electrical Resistivity and Magnetic Properties. *Inorg. Chem. Commun.*, 149(August 2022): 110452. https://doi.org/10.1016/j.inoche.2023.110452

Wang, Jialing, Sun, Aimin, Jiang, Ying, Huang, Xiaoyan, Shao, Liqiong and Zhang, Yanchun (**2022**), Structural and Magnetic Properties of Ce3+doped Mg-Co Ferrite Prepared by Sol–Gel Method. *J. Mater. Sci. Mater. Electron.*, 33(15): 11881–11895. https://doi.org/10.1007/s10854-022-08150-8

Yonatan Mulushoa, S., Murali, N., Tulu Wegayehu, M., Veeraiah, V. and Samatha, K. (**2018**), Investigation of Structural, DC-Resistivity and Magnetic Properties of Mg Ferrite. *Mater. Today Proc.*, 5(13): 26460–26468. https://doi.org/10.1016/j.matpr.2018.08.100

قياسات تحويل فوريبه للطيف بالأشعة تحت الحمراء (FTIR) و التوصيلية الكهربية للمغنيسيوم نانوفريت ومركباتها مع أكسيد الجرافين المختزل (rGO) والبولي بيرول (PPy).

بلال ابراهيم، مها خالد، سامية سعفان، رضا الشاطر

جامعة طنطا، كلية العلوم، قسم فيزياء

تم تحضير جزيئات الفريت النانومترية باستخدام تقنية الاحتراق الذاتي لسلائف السترات. كما تم تحضير بولمير البولي بيرول (PPy) بتقنية البلمرة الكيميائية لمونومر البيرول. بالإضافة إلى ذلك تم تحضير متراكبات عن طريق خلط الفريت المحضر مع بوليمر البولي بيرول (PPy) و/أو أكسيد الجرافين المختزل (rGO) بنسب مختلفة. كما تم التأكد من الخصائص الهيكلية للعينات النانومترية بواسطة حيود الأشعة السينية (XRD) ووجد أن ثابت الشبكة البلورية يساوي ٨٤٥.٠ أنجستروم ومتوسط الحجم البلوري ٤٠ نانومتر. علاوةً على ذلك تم استخدام مطيافية الاشعة تحت الحمراء (FTIR) للتأكد من بنية وطور جميع العينات والمتراكبات المحضرة وأظهرت الأوضاع الاهتزازية موضع ثماني السطوح عند ٤٠٥ سم$^{-1}$ وموضع رباعي السطوح عند ٥٦٥ سم$^{-1}$ المميزين لبنية الإسبنيل. أثبت تحليل مطيافية تشتت الطاقة بالأشعة السينية (EDX) عن وجود عناصر الحديد والمغنيسيوم والأكسجين والكربون والنيتروجين مما يشير إلى نقاء التركيب الكيميائي للفريت ومتراكباته. تم قياس موصلية التيار المستمر لجميع العينات كدالة في درجة الحرارة. تُظهر عينة (الفريت/ والبولي بيرول) موصلية أكبر للتيار المستمر مقارنة بعينة (الفريت النقية) وعينة (الفريت/ وأكسيد الجرافين المختزل). بينما يُظهر متراكب (فريت المغنسيوم/ ١٠% بولي بيرول/ ١٠% أكسيد الجرافين المختزل) موصلية استثنائية بسبب تفاعل التراص القوي π-π بين أكسيد الجرافين المختزل والبولي بيرول. يسمح هذا التفاعل بتوليد عدد أكبر من الإلكترونات غير المتمركزة داخل بنيتها، وبالتالي تقليل العوائق التي تعترض حركة الإلكترون وتسهيل تدفق الإلكترونات بسهولة أكبر. علاوة على ذلك، فبداخل هذا المركب -الذي يشتمل على البولي بيرول وأكسيد الجرافين المختزل- تكون هذه التأثيرات واضحة بشكل خاص. ولذلك، فإن متراكب (فريت المغنسيوم/ ١٠% بولي بيرول/ ١٠% أكسيد الجرافين المختزل) يمتلك أصغر طاقة تنشيط بين جميع العينات (والتي تساوي ١٤٥.٠ إلكترون فولت).